ENHANCING URBAN DIGITAL ELEVATION MODELS USING AUTOMATED COMPUTER VISION TECHNIQUES

B. Sirmacek, P. d'Angelo, T. Krauss, P. Reinartz

German Aerospace Center (DLR), Remote Sensing Technology Institute
PO Box 1116, 82230, Wessling, Germany
(Beril.Sirmacek, Pablo.Angelo, Thomas.Krauss, Peter.Reinartz)@dlr.de

Commission VII

KEY WORDS: Urban, Modelling, Detection, DEM/DTM, Cartosat-1

ABSTRACT:

In recent years Digital Elevation Models (DEM) gained much interest because of their high capability to give information about urban regions. DEM can be used for detailed urban monitoring, change and damage detection purposes. However, initially a DEM with very sharp details should be constructed. The DEM can be derived from very high resolution stereo satellite images, but for most of the cases just one stereo pair is available. Unfortunately after this process, regions which are occluded in one of the stereo images have no height value in the DEM data. This is a major problem especially in urban DEM, since many regions are occluded by buildings. However these occluded regions can be filled using interpolation techniques, which lead to lose sharpness in building edges. Besides due to low resolution of input stereo images, the generated DEM resolution can be too low to represent buildings.
In order to increase details, herein we propose a special automated urban DEM enhancement technique. To do so, first we detect possible building locations using height information of the DEM. Then using corresponding panchromatic image, we detect building shapes with an automatic shape approximation approach. Using detected building shapes, we refine buildings in the DEM. Finally, for a better representation we locate constructed three-dimensional building models on Digital Terrain Model (DTM) of the corresponding region. We believe that the implemented enhancement will not only provide better three-dimensional urban region representation, but also will lead to more detailed change and damage investigation in future studies.

1 INTRODUCTION

An important research field in remote sensing is three-dimensional analysis and reconstruction of urban objects. Especially urban monitoring, damage assessment, and disaster monitoring fields need to achieve realistic three-dimensional urban models. A rather new technology in this context is the Digital Elevation Model (DEM) generation based on stereo image matching principle using satellite data. Unfortunately, there are several problems in generated DEM. First, regions which are occluded in one of the stereo images have no height value in DEM data. Interpolation techniques, which are used to fill these non-value regions, lead to lose sharpness in building edges. Generated DEM have limited resolution and raw DEM data may not represent buildings correctly. In addition to that, DEM does not provide intensity and color information. Therefore, some advanced processes are required to enhance the DEM.

In literature, many researchers developed techniques for DEM enhancement. A considerable amount of these studies has been published on reducing errors in DEM which generally belong to rural regions (Skarlatos and Georgopoulos, 2004, Ostrowski and He, 1989). In recent years, three-dimensional modeling of urban regions gained great interest. Thus, some of the researchers focused on enhancing urban DEM data for better urban region representation. Haala et al. (Haala et al., 1998) proposed a method to reconstruct building rooftops using surface normals extracted from DEM data. They assumed that building boundaries are detected previously. In a following study (Haala and Brenner, 1999), they detected building boundaries automatically by classification DEM and corresponding color image before applying their automatic rooftop reconstruction method. Brunn and Weidner (Brunn and Weidner, 1997) used surface normals on DEM to discriminate buildings and vegetation. After extracting buildings, they measured geometry of rooftops using surface normals and they interpolated polyhedral building descriptions to these structures. Fradkin et al. (Fradkin et al., 1999) proposed segmentation based method to reconstruct three-dimensional models of dense urban areas. To this end, they used very high resolution color aerial images and DEM data. Canu et al. (Canu et al., 1996) used high resolution DEM to reconstruct three-dimensional buildings. First, they segmented DEM into homogeneous regions. Then, they interpolated flat surfaces on these regions. Ortner et al. (Ortner et al., 2002) used point process to model urban areas. They represented urban areas as interacting particles where each particle stands for an urban object. Preknowledge about building shapes is used to model these particles. Arefi et al. (Arefi et al., 2008) extracted above-ground objects from LIDAR data. Then, three-dimensional buildings are reconstructed by hierarchical fitting of minimum boundary rectangles (MBR) and RANSAC based straight line fitting algorithm. In these studies, good results are achieved generally using very high resolution (more than 1 m. spatial resolution) DEMs which are generated from airborne data sets. However, enhancement of buildings in very low resolution urban DEM data which is generated from satellite images is still an open research problem. As a different approach, Elaksher (Elaksher, 2008) proposed a multi-photo least squares matching based DEM enhancement method. They detected discontinuities in a least squares matching model. Using multiple photos of a region, they applied a least squares matching process recursively until the refinement is sufficient. However, the proposed method can smooth noises and enhance details in very coarse DEM data, it needs multiple photos of the same region taken from different looking angles which is generally difficult to obtain, especially from satellites.

In another study, Vinson et al. (Vinson et al., 2001, Cohen and Vinson, 2002) developed an approach for detecting rectangular buildings in DEM. For this purpose, they segmented above ground objects in the DEM. Then, they tried to model each above ground

segment by a rectangle. They used estimated rectangular shapes to enhance building representation in DEM. Herein, we provide a fast and fully automatic approach to enhance DEM data based on building shape approximation. For this purpose, first we extract above ground objects in DEM. Since our DEM data are in very low resolution (in 5 m. spatial resolution), it is not convenient to extract building shapes. Therefore different from Vinson et al., we detect building shapes from panchromatic image of region. To detect building shapes, we benefit from automatic rectangular shape approximation approach (Box-Fitting) (Sirmacek and Unsalan, 2008). Finally, using detected building shapes we refine the DEM data. For a better representation, we also reconstruct building shapes on interpolated and smoothed Digital Terrain Model (DTM) of the corresponding region. The resulting enhanced three-dimensional data will not only provide better visual result, but also will provide a basis for detailed three-dimensional modeling and change detection analysis.

2 DETECTING BUILDING LOCATIONS USING DEM AND DISTANCE TRANSFORM

In a previous study, d'Angelo et al. proposed a fully automated method to generate DEM (d'Angelo et al., 2009). For this purpose, they applied hierarchical intensity based matching, and then dense epipolar matching to stereo images with 2.5 m. ground sampling distance (GSD) taken from the Cartosat-1 satellite. Looking angle differences of two satellite images are about 31°, which is too much higher than normally wanted to reconstruct buildings. Normally, 10° angle difference between stereo image pairs is wanted to reconstruct buildings. Unfortunately, it is very difficult to obtain stereo image couples with this small looking angle from satellite images. In another study, Arefi and Hahn (Arefi and Hahn, 2005) proposed a DTM generation method from LIDAR based on geodesic dilation. Then, Arefi et al. (Arefi et al., 2009) developed the algorithm for DTM generation from DEM. Herein, we use DEM and DTM data which are generated using methods of d'Angelo et al. and Arefi et al. which are reported in (d'Angelo et al., 2009) and (Arefi et al., 2009) respectively.

The difference between DEM and DTM is known as normalized Digital Elevation Model (nDEM). In the normalized DEM ground height is referenced to zero, therefore it provides information about approximate building heights independent from the terrain. To estimate urban areas, we first generate nDEM ($N(x,y)$) by taking difference of DEM ($E(x,y)$) and DTM ($T(x,y)$) image matrices which belong to the same region. Then, we apply Otsu's automatic thresholding method to detect urban area in $N(x,y)$ (Otsu, 1979). After applying thresholding, we assume output $M(x,y)$ binary image as urban area mask which holds K number of binary subregions. In order to eliminate effect of trees, we analyze each $M_k(x,y)$ $k \in [1,2,...,K]$ subregion in $M(x,y)$ urban area mask. If $\max(N(x,y) \times M_k(x,y))$ is smaller than 2 meters, we eliminate $M_k(x,y)$ subregion since it is not high enough to represent a building. In Fig. 1(a), we represent $Jedda_1$ test image from our data set, and in Fig. 1(b) we show detected urban area boundaries.

After finding the urban area from the DEM, we label buildings in order to model each of them with a rectangular shape. Unfortunately, due to very low resolution of this DEM and high complexity of the region, it is not possible to always distinguish adjacent buildings from DEM data. Therefore we pick panchromatic image of region ($I(x,y)$) for further analysis. First, we apply a preprocess to $I(x,y)$ image using bilateral filter which performs a non-linear smoothing with preserving edge information (Tomasi and Manduci, 1998). In this way, we eliminate noise and redundant details in image. Sirmacek and Unsalan provides an extensive explanation about usage of bilateral filter in panchromatic satellite images (Sirmacek and Unsalan, 2009). To find buildings, we benefit from Canny edges (Canny, 1986). We extract Canny edges of $I(x,y)$ test image, then we use $M(x,y)$ urban area mask to obtain only building edges. For our $Jedda_1$ sample test image, detected building edges can be seen in Fig. 1(c). Then, we use distance transform to find a location inside of each closed building edge shape. For binary images (like our building edges in Fig. 1(c)), distance transform calculates the distance between each pixel that is set to zero and the nearest nonzero pixel. In our study, we use *Euclidean Distance* as distance metric. After applying distance transform to our building edges, centers of building shapes get highest values. Consequently, we pick local maximum values in distance transform, and assume their locations (x_b, y_b) as possible building centers. In Fig. 1(d) we represent detected building locations for our $Jedda_1$ test image. As can be seen in this figure, most of the buildings are labeled correctly. Next, we describe the proposed automatic building shape approximation method.

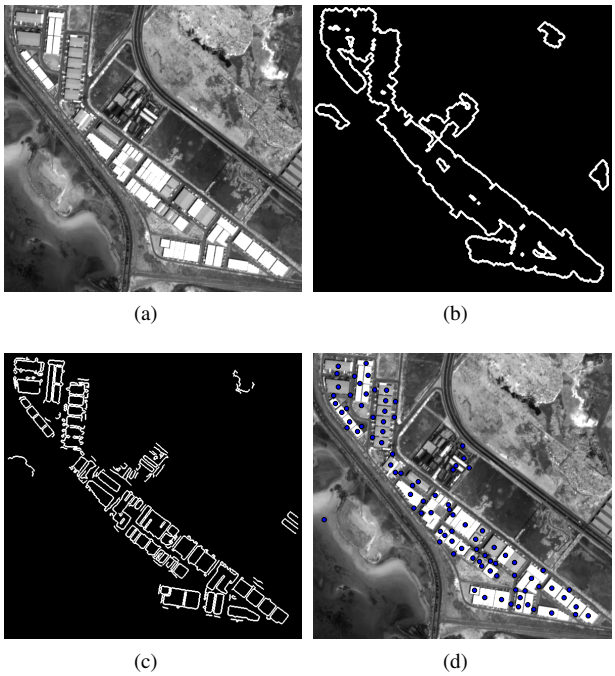

(a) (b) (c) (d)

Figure 1: (a) $Jedda_1$ test image. (b) Detected urban area boundaries. (c) Canny edges detected in urban area. (d) Possible building centers (x_b, y_b).

3 EXTRACTING BUILDING SHAPES (BOX-FITTING)

In complex urban areas which contain adjacent buildings, very low resolution DEM data can not be used for detecting shapes of buildings. Therefore, we use Canny edges which are extracted from panchromatic image to estimate building shapes. In a previous study Sirmacek and Unsalan (Sirmacek and Unsalan, 2008) proposed an automatic shape approximation approach (called Box-Fitting) after a seed-point is detected on the building rooftop. In this study, we benefit from this Box-Fitting approach to detect approximate building shapes. We assume (x_b, y_b) possible building centers as seed-points to run Box-Fitting algorithm.

To estimate building shapes for each (x_b, y_b) location, we locate a $[w \times w]$ size window on this building center. Considering resolution and approximate building sizes in our test images, we assume w as equal to 60 pixel. Box-Fitting method discards edges

out of this window to deal only with candidate building edges and to decrease the number of unnecessary edges. From these edges, the rectangle that represents the building is reconstructed. For each possible building location, we put an initial virtual box on (x_b, y_b) coordinate with $\theta = 0$ angle. Here, θ is the slope of the rectangle. Then, the edges belonging to the virtual box are swept outwards, until they hit to building edges. After our virtual box stops growing, we calculate the energy E_θ. The energy of the detected box shape is defined as the sum of minimum distance between virtual building edge pixels and real building edge pixels in perpendicular direction as given below;

$$E_\theta = \sum_{i=1}^{n} min(sqrt((x_v(i) - x_e(j))^2 - (y_v(i) - y_e(j))^2)) \quad (1)$$

Here, E_θ is the calculated energy in θ direction. $(x_v(i), y_v(i))$ represent coordinates for ith pixel on the edges of the virtual box shape. $(x_e(j), y_e(j))$ represents the jth pixel on the real building edges. For same seed-point, we put an initial virtual box and start growing again for all $\theta \in [0, \pi/6, \pi/3, \pi/2, 2\pi/3, ..., 2\pi]$ angles. As we increase step sizes here, we can obtain more accurate approximations, however we need more computation time. After calculating E_θ for $\theta \in [0, \pi/6, \pi/3, \pi/2, 2\pi/3, ..., 2\pi]$ angles, we pick the estimated box which has smallest E_θ energy as detected building shape. Since buildings are generally in rectangular shapes, it makes sense to extract rectangular shapes on buildings. Main advantage of using Box-Fitting approach is that approximate building shape still can be found even the building edges are not well-determined, or even if there is not a closed shape. However, other region growing algorithms fail to extract an object shape in these cases.

In Fig. 2, we represent our original $Jedda_1$ sample image, and $B(x, y)$ binary image which holds detected approximate building shapes. As one outcome of using the Box-Fitting approach, we can reject some false seed-points if the virtual box can not converge to a shape in this region. We also reject the detected box-shape if its area is very small (less than 100 pixels), or if its area is very large (more than 5000 pixels) since it can not represent a real building considering image resolutions. As a result, we also verify building appearance using Box-Fitting algorithm. In the next part, we use detected approximate building shapes to refine the DEM.

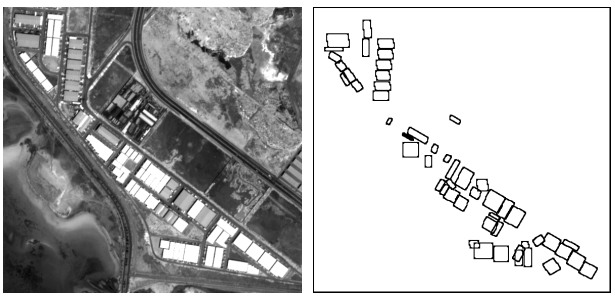

(a) (b)

Figure 2: (a) Original $Jedda_1$ test image. (b) Detected approximate shapes using box-fitting approach ($B(x, y)$ binary image).

4 ENHANCING BUILDING SHAPES IN DEM

After finding approximate building shapes from the panchromatic satellite image, we try to enhance DEM data using this information. For this purpose, we first calculate gradient magnitudes in DEM to investigate discontinuities. To find gradient magnitudes, we use smoothed gradient filters in x and y directions as below,

$$g_x(x, y) = \frac{-x}{2\pi} exp(-\frac{x^2 + y^2}{2\sigma^2}) \quad (2)$$

$$g_y(x, y) = \frac{-y}{2\pi} exp(-\frac{x^2 + y^2}{2\sigma^2}) \quad (3)$$

where σ is the smoothing parameter and equal to 0.5. Although our method is fairly robust to this parameter, one may need to adjust it according to the resolution of DEM. We calculate the smoothed gradients for the DEM data $E(x, y)$ as,

$$E_x(x, y) = g_x(x, y) * E(x, y) \quad (4)$$

$$E_y(x, y) = g_y(x, y) * E(x, y) \quad (5)$$

where $*$ stands for a two-dimensional convolution operation. We calculate gradient magnitudes of image as,

$$G(x, y) = \sqrt{E_x(x, y)^2 + E_y(x, y)^2} \quad (6)$$

If a pixel in $G(x, y)$ has a higher value than t_d, we assume there is a significant discontinuity. Here, t_d threshold value is obtained by Otsu's automatic thresholding approach (Otsu, 1979). After detecting significant discontinuities in the DEM, we pick each rectangle and investigate the corresponding region. If there are discontinuities in the DEM pixels where rectangle have edges, we assume the inside of this rectangle as a building rooftop. In order to eliminate noise that appears on building rooftops, we calculate only one height for each rectangular building. To calculate an approximate building heights, we pick DEM values which are inside of the detected rectangular region and calculate their mean value. Then we set each pixel, which exists inside of the rectangular region, to the calculated mean value. As a result, we have only one height value for each detected building. In the Experimental Results section, we analyze effects of choosing mean and median of DEM values as a building height.

We assume that there may be buildings in the DEM which are missed in previous building detection and shape approximation steps. Therefore, after removing reconstructed building pixels from DEM we make a post-analysis on it. If there are regions with high values for a large area, we assume that they can be missed buildings and insert them to our final result after smoothing their DEM values with a $[9 \times 9]$ size median filter to remove the noise on DEM. We picked this median filter window size after extensive tests on our test image dataset. If window size is chosen larger, this post-processed buildings will have smoother edges. On the other hand, if window size is chosen smaller, median filtering process can not be adequate to remove noise within DEM. In this post-analysis, if a region has very high value (more than 40 meters) we remove this region from DEM since it can not represent a building. In this way, we also eliminate errors in the DEM which occur because of stereo image matching errors in the DEM generation process.

5 EXPERIMENTAL RESULTS

To test the performance of our proposed method, we use a test image data set of Jedda city. We use DEM which is generated from

stereo Cartosat-1 images using the DEM generation method of d'Angelo et al. (d'Angelo et al., 2009). We also use orthorectified panchromatic Cartosat-1 image of the corresponding region. For better representation, we locate reconstructed buildings on a smoothed DTM of the region which is generated using method of Arefi and Hahn (Arefi and Hahn, 2005). Our panchromatic Cartosat-1 test images have 2.5 m. spatial resolution, however DEM and DTM have 5 m. spatial resolution.

In the first row of Fig. 3, we represent the orthorectified panchromatic Cartosat-1 image, the original DEM, and the enhanced DEM for our $Jedda_1$ sample test image respectively. For a better visual representation we covered the DEM with the panchromatic image of the region. In the second row of Fig. 3, we represent another example from our test image dataset. In this row, we represent the orthorectified panchromatic Cartosat-1 image, the original DEM, and the enhanced DEM for our $Jedda_3$ test image. As can be seen in these examples, the enhanced DEM data reflects building reconstruction in urban area more clearly. Besides, DEM errors which come from automatic the DEM generation method are also corrected in the enhanced DEM. However, we could not detect exact shapes of complex buildings and we can not discriminate some of the adjacent buildings, the final improvement in DEM data is informative. We will analyze detection of complex building shapes in our future studies. Next, we analyze performance of our proposed method on a sample test image to give a sight to possible readers.

5.1 Performance Analysis on Sample Image

We pick $Jedda_1$ test image to evaluate the performance of our method. To analyze performance we consider two measures; shape accuracy (p_1) and height accuracy (p_2). First, we start with measuring shape accuracy of the shape approximation (Box-Fitting) approach. We use the method used by Ruether et al. (Ruether et al., 2002) to measure the shape accuracy. For a $[m \times n]$ size test image shape accuracy performance (p_1) is calculated as follows,

$$p_1 = \left(\frac{\sum_{x=1}^{m}\sum_{y=1}^{n}|B_f(x,y) - B_{gth}(x,y)|}{\sum_{x=1}^{m}\sum_{y=1}^{n}B_{gth}(x,y)}\right) \times 100 \quad (7)$$

in this equation $B_f(x,y)$ is the binary image which is obtained by filling holes as '1' in $B(x,y)$ binary image. B_{gth} is the binary groundtruth shape mask that we labeled buildings as '1' and other regions as '0' manually. We calculate p_1 value as $78,02\%$ for $Jedda_1$ test image. Unfortunately, 53 of 66 buildings are detected in the region. Therefore, our groundtruth masks includes some buildings which are not detected in building shape detection method, so those buildings are not labeled after our shape approximation method. Therefore, we obtain slightly low shape accuracy performance. If shape accuracy is calculated for each building one by one, we can observe higher shape accuracy performance for each building.

In order to calculate height accuracy, we first calculate each building height in $Jedda_1$ test image using panchromatic stereo CartoSat-1 images. Using triangulation techniques, we measure each building height manually and list obtained height values as vector data. We also list building heights in the same order measuring the heights in the final enhanced DEM data. We generated enhanced DEM both using mean and median values of building rooftop values. As a result, two enhanced DEM building height value vectors are used in performance calculation. By subtracting groundtruth building height vector from these vectors, the differences can be obtained. In the ideal case, we expect to obtain zero values as difference. In order to measure height accuracy (p_2), we used RMS values of these difference vectors. For the vector generated by using the mean of DEM values, RMS of difference vector is calculated as 1.80. For the vector generated by using the median of DEM values, RMS of difference vector is calculated as 2.63. We pick the method which generates p_2 value closer to zero. Therefore, using mean value of DEM when calculating building heights gives more accurate results.

5.2 Computation Times

We finally analyze computation time needed for our method. The computation time of the proposed DEM enhancement method is also very impressive. For our sample $Jedda_1$ test image which is in $[566 \times 590]$ pixel sizes, we tabulate timing requirements of all modules in the DEM enhancement method in Table 1. We obtain these timings using an Intel Core2Quad 2.66GHz PC and Matlab coding environment. As can be seen in this table, segmenting urban area from DEM data requires only 0.28 seconds. We detect possible building locations in 1.74 seconds. The longest computation time is needed for shape approximation (Box-Fitting) step. For $Jedda_1$ test image which includes 76 buildings, shape approximation step requires 65.14 seconds. In this step, timing directly depends on the test image. As the number of buildings increases in given test image, the shape approximation module needs more computation time. However, this module can run faster if it is coded in C. Finally, enhancing building shapes in DEM requires 0.82 seconds. Consequently, running our proposed DEM enhancement method on $Jedda_1$ test image requires 67.98 seconds. This short computation time may lead for the proposed method to be used in fast damage and change detection applications.

Unfortunately, our method is not able to detect exact shapes of very complex buildings. Therefore, edges of these buildings are not sharpened in DEM data. We will handle detection of complex building shapes in our future studies.

Module	Time (in Sec.)
Urban area segmentation	0.28
Detecting buildings	1.74
Shape approximation (Box-Fitting)	65.14
Enhancing building shapes	0.82
TOTAL	67.98

Table 1: CPU Times (In Seconds) for DEM Enhancement on $Jedda_1$ test image

6 CONCLUSIONS

In this paper, we proposed a new method for automatic DEM enhancement based on building shape approximation. First, we detected the urban area using DEM. Then, we used panchromatic image of corresponding region to detect possible building centers. For this purpose, we extracted Canny edges of buildings in the previously detected urban area. After that, we applied distance transform to these edges to detect building centers. We used detected edges and building centers to run the shape approximation algorithm. Extracted approximate shapes helped us to sharpen building edges, and to smooth rooftops in the DEM. We also corrected errors in DEM, which appear due to stereo image matching errors in DEM generation.

After extensive tests on very low resolution and noisy DEMs, we obtained encouraging results with our method. Comparing with

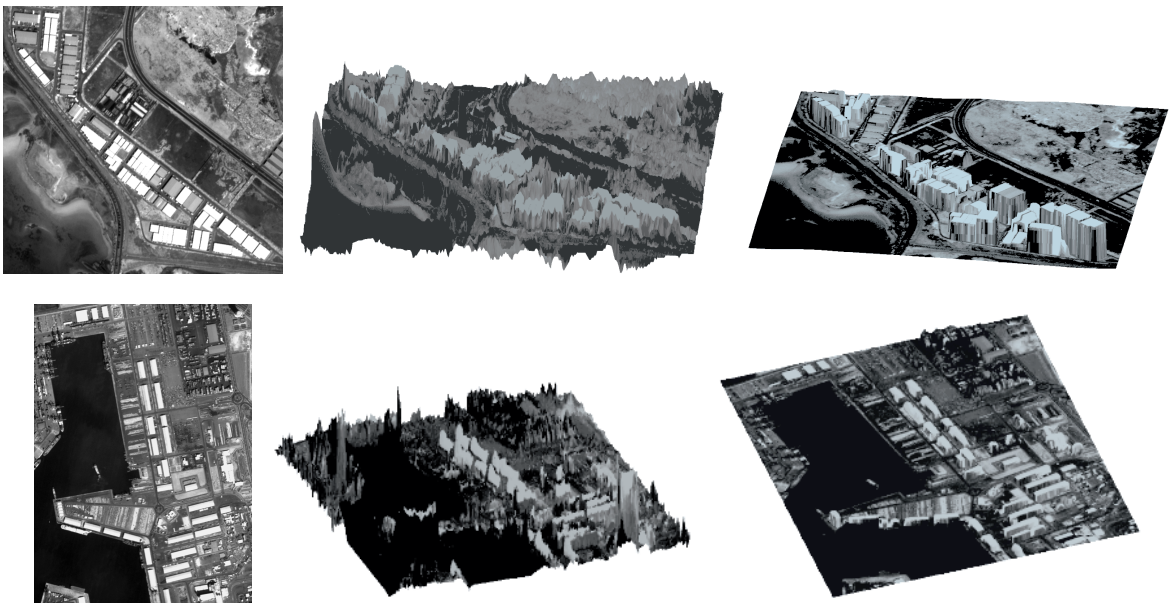

Figure 3: Orthorectified pancromatic Cartosat-1 images, original DEM, and enhanced DEM are given in each raw for $Jedda_1$, and $Jedda_3$ test regions respectively.

studies presented in the literature, we can conclude that our proposed urban DEM enhancement method is fast and reliable even in complex urban regions. The proposed automatic method will decrease operator work-loads in three-dimensional reconstruction of urban areas. In addition to that, we believe that proposed method will be of use for detailed urban monitoring, damage and change detection systems. The next step of this study will be the detection of more complex building shapes and textured rooftops.

REFERENCES

Arefi, H. and Hahn, M., 2005. A morphological recontruction algorithm for separating off-terrain point. In Proceedings of the International Archives of Photogrammetry, Remote Sensing, and Spatial Information Sciences 46, pp. 1–6.

Arefi, H., d'Angelo, P., Mayer, H. and Reinartz, P., 2009. Automatic generation of digital terrain models from cartosat-1 stereo images. In Proceedings of the International Archives of the Photogrammetry, Remote Sensing and Spatial Information Sciences.

Arefi, H., Engels, J., Hahn, M. and Mayer, H., 2008. Levels of detail in 3d building reconstruction from lidar data. In Proceedings of the International Archieves if the Photogrammetry, Remote Sensing, and Spatial Information Sciences 37, pp. 485–490.

Brunn, A. and Weidner, U., 1997. Extracting buildings from digital surface models. In Proceedings of International Archives of Photogrammetry, Remote Sensing, and Spatial Information Sciences.

Canny, J., 1986. A computational approach to edge detection. IEEE Transactions on Pattern Analysis and Machine Intelligence 8 (6), pp. 679–698.

Canu, D., Gambotto, J. and Sirat, J., 1996. Reconstruction of building from multiple high resolution images. In Proceedings of International Conference on Image Processing.

Cohen, L. and Vinson, S., 2002. Segmentation of complex buildings from aerial images and 3d surface reconstruction. In Proceedings of 6th IEEE Workshop on Applications of Computer Vision (WACV) 1, pp. 215–219.

d'Angelo, P., Schwind, P., Krauss, T., Barner, F. and Reinartz, P., 2009. Automated dsm based georeferencing of cartosat-1 stereo scenes. In Proceedings of International Archives of Photogrammetry, Remote Sensing, and Spatial Information Sciences.

Elaksher, A., 2008. A multi-photo least squares matching algorithm for urban area dem refinement using breaklines. In Proceedings of International Archives of Photogrammetry, Remote Sensing, and Spatial Information Sciences 37, Part B3A, pp. 33–38.

Fradkin, M., Roux, M., Maitre, H. and Leloglu, U., 1999. Surface reconstruction from multiple aerial images in dense urban areas. In Proceedings of IEEE Computer Vision and Pattern Recognition 2, pp. 262–267.

Haala, N. and Brenner, C., 1999. Extraction of buildings and trees in urban environments. ISPRS Journal of Photogrammetry and Remote Sensing 54, pp. 130–137.

Haala, N., Brenner, C. and Anders, K., 1998. 3d urban gis from laser altimeter and 2d map data. In Proceedings of International Archives of Photogrammetry, Remote Sensing, and Spatial Information Sciences 32, pp. 339–346.

Ortner, M., Descombes, X. and Zerubia, J., 2002. Building extraction from digital elevation models. INRIA Research Report.

Ostrowski, J. and He, D., 1989. Error correction of digital elevation models produced by automatic matching of digital stereo images. In Proceedings of International Geoscience and Remote Sensing Symposium (IGARSS) 2, pp. 446–449.

Otsu, N., 1979. A threshold selection method from gray-level histograms. IEEE Transactions on Systems, Man, and Cybernetics 9 (1), pp. 62–66.

Ruether, H., Martine, H. M. and Mtalo, E., 2002. Application of snakes and dynamic programming optimisation technique in modelling of buildings in informal settlement areas. ISPRS Journal of Photogrammetry and Remote Sensing 56 (4), pp. 269–282.

Sirmacek, B. and Unsalan, C., 2008. Building detection from aerial imagery using invariant color features and shadow information. In Proceedings of International Symposium on Computer and Information Sciences (ISCIS) 1, pp. 1–5.

Sirmacek, B. and Unsalan, C., 2009. Urban-area and building detection using sift keypoints and graph theory. IEEE Transactions on Geoscience and Remote Sensing 47 (4), pp. 1156–1167.

Skarlatos, D. and Georgopoulos, A., 2004. Automating the checking and correcting of dems without reference data. In Proceedings of International Archives of Photogrammetry, Remote Sensing, and Spatial Information Sciences 35, Part B2, pp. 553–558.

Tomasi, C. and Manduci, R., 1998. Bilateral filtering for gray and color images. In Proceedings of International Conference on Computer Vision 1, pp. 839–846.

Vinson, S., Cohen, L. and Perlant, F., 2001. Extraction of rectangular buildings in aerial images. In Proceedings of Scandinavian Conference on Image Analysis (SCIA'01).